

DOI 10.24425/ae.2022.141679

Modelling of synchronous generators for the analysis of frequency transients above 1 Hz/s

ALF ASSENKAMP

Bureau Veritas CPS Germany GmbH
Germany

e-mail: assenkamp@gmx.de

(Received: 04.09.2021, revised: 11.04.2022)

Abstract: Large synchronous generators are of high importance for the stability of power systems. They generate the frequency of the system and stabilize it in case of severe grid faults like trips of large in-feeders or loads. In distributed energy systems, in-feed via inverters will replace this generation in large parts. Modern inverters are capable of supporting grid frequency during severe faults by different means on the one hand. On the other hand, higher Rates of Change of Frequency (RoCoF) after incidents need to be accustomed by future systems. To be able to analyse the RoCoF withstand capability of synchronous or induction generators, suitable models need to be developed. Especially the control and excitation system model need enhancements compared to models proposed in standards like IEEE Std 421.5. This paper elaborates on the necessary modelling depth and validates the approach with example results.

Key words: control system, distributed energy systems, frequency support, generator model, RoCoF, synchronous generators, synchronous machines

1. Introduction

In recent years, it has become increasingly important to carry out electromagnetic transient studies on generators in electrical networks. One reason is that due to the energy transition the amount of distributed energy resources increases. The current European Requirements for Generators [1] place high demands on the generators, such as the ability to stay connected during events with high RoCoF.

In addition, more and more grid connection rules also require grid support from new generators for permission to feed into the grid [2]. A good overview on state-of-the-art techniques of wind farms to support grid frequency is given in [3].



© 2022. The Author(s). This is an open-access article distributed under the terms of the Creative Commons Attribution-NonCommercial-NoDerivatives License (CC BY-NC-ND 4.0, <https://creativecommons.org/licenses/by-nc-nd/4.0/>), which permits use, distribution, and reproduction in any medium, provided that the Article is properly cited, the use is non-commercial, and no modifications or adaptations are made.

The link between the stator and rotor is represented by the electromechanical torque T_{el} . Dependencies of T_{el} can be seen in the following expression [18]:

$$T_{el} = \frac{d}{d\varphi} \sum_{j=0}^n \sum_{k=0}^m \left(L_{j,k}^{S,R}(\varphi) \cdot i_j^S(t) \cdot i_k^R(t) \right), \quad (1)$$

where: φ is the rotation angle of the rotor, $L_{j,k}^{S,R}$ is the coupling inductance of the rotor winding k and the stator winding j , i_j^S is the current in the stator winding j , i_k^R is the current in the rotor winding k , n is the number of the stator currents, m is the number of the rotor currents.

There is a strong dependence between the different terms of Eq. (1). Any change in the load or feed steady state situation of the power system leads directly to changes in the electromechanical torque T_{el} , rotor and stator currents i_k^R , i_j^S , rotation angle φ , angular velocity $\dot{\varphi}$, and coupling inductances $L_{j,k}^{S,R}$. The system oscillates until it returns to a stable state.

2.2. RoCoF definition

RoCoF is defined as the rate of change of frequency Δf over a given time period Δt :

$$\text{RoCoF} = \frac{\Delta f}{\Delta t}. \quad (2)$$

It is important to point out, that the RoCoF value measured depends strongly on the location within the power system, especially for large systems. Interesting study outcomes on this topic are presented in [7].

To answer the question, how this frequency gradient looks like for realistic events, Fig. 2 depicts results of the simulation of a loss of a large generator within a system dominated by

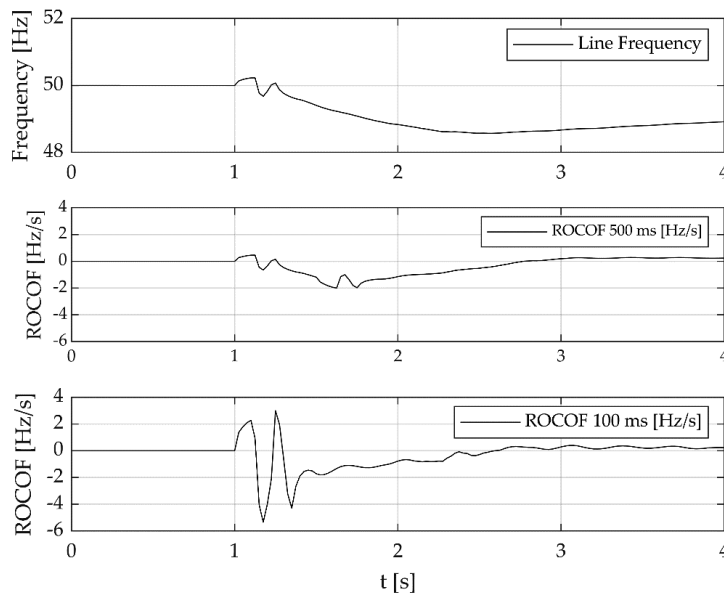


Fig. 2. Typical frequency excursion after trip of load

synchronous generation. The fault occurs at $t = 1$ s. The RoCoF depicted is measured with a rolling measuring window of $\Delta t = 100$ ms and $\Delta t = 500$ ms, respectively, to show the influence of the measuring window on the resulting RoCoF value.

Directly after the fault, the system frequency increases and decreases quickly several times with a high RoCoF. This flickering of the grid frequency is not what is expressed in the time independent formulation of Eq. (18), but only direct consequences of the fault before the fault energy is being compensated by a frequency gradient.

It can be seen, that between $t = 1.4$ s and $t = 2.0$ s, the frequency gradient is almost linear. This is the time span, where the turbine governors of the synchronous generators did not have time to adapt power output to the new load situation. In this situation, the fault energy is being transferred almost completely from rotational energy of the synchronous generators.

After $t = 2.5$ s simulation time, frequency starts increasing and the system begins to return to normal operation.

2.3. RoCoF in power systems with high inertia

When the disturbance is severe enough so that electrical quantities throughout the power system oscillate for several seconds, it is a transient disturbance of the system. One measure for the severance of the disturbance is the Rate of Change of Frequency (RoCoF) resulting from the disturbance at a certain location.

For a power system with mainly synchronous generation directly coupled to the system, it is possible to derive a simple formula for the initial RoCoF rate directly after the event.

Therefore, the assumption is that the energy of the fault transfers directly to rotational energy of the synchronized generators [6]:

$$E_{\text{fault}} \rightarrow \Delta E_{\text{rot}} = \Delta \frac{1}{2} J(\omega)^2, \quad (3)$$

where: ω is the angular velocity, is the sum of the inertia of the shaft trains of directly coupled power plants, E_{rot} is the rotational energy, E_{fault} is the energy of failure.

This assumption neglects any losses within the system as well as time dependencies. At the same time, it can be seen directly that loss of generation leads to decreasing rotational energy and thus decreasing system frequency, and loss of load leads to increasing system frequency.

To define the fault energy E_{fault} , the power change due to the fault P_{fault} is defined as a momentary difference between generation and load:

$$P_{\text{fault}} = P_{\text{generation}} - P_{\text{load}} = \Delta P. \quad (4)$$

The time derivative of the fault energy E_{fault} consequently results in:

$$P_{\text{fault}} \approx \frac{d}{dt} E_{\text{rot}} = \frac{d}{dt} \left(\frac{1}{2} J_{\text{grid}} \omega_{\text{grid}}^2 \right). \quad (5)$$

In Eq. (4), J_{grid} is the inertia sum for directly coupled synchronous generators in the system. The inertia constant of the entire shaft train, which is determined as the sum of the mass moments

of inertia of the generator and the turbine, $H_{\text{shaft train}}$, is defined as the kinetic energy of the shaft train $J_{\text{shaft train}}$ divided by its rated apparent power. For a generator with p pole pairs it is consequently:

$$H_{\text{shaft train}} = \frac{J_{\text{shaft train}} \omega_{\text{grid}}^2}{2p^2 S_{\text{shaft train}}} . \quad (6)$$

In conventional power systems, generators with $p = 1$ dominate the system:

$$H_{\text{shaft train}} = \frac{J_{\text{shaft train}} \omega_{\text{grid}}^2}{2 S_{\text{shaft train}}} . \quad (7)$$

The rotational energy of the system can consequently be written as:

$$E_{\text{rot}} = H_{\text{grid}} S_{\text{grid}} = \sum H_{\text{shaft train}} S_{\text{shaft train}} . \quad (8)$$

Dividing Eq. (4) by rated apparent power of the whole system S_{grid} leads to the related power change:

$$\bar{P}_{\text{fault}} = \frac{d}{dt} \frac{\sum H_{\text{shaft train}} S_{\text{shaft train}}}{S_{\text{grid}}} \bar{\omega}_{\text{grid}}^2 . \quad (9)$$

In (8), $\bar{\omega}_{\text{grid}}^2$ is the related angular velocity. As the next step, H_{grid} from Eq. (7) is inserted:

$$\bar{P}_{\text{fault}} = \frac{d}{dt} H_{\text{grid}} \bar{\omega}_{\text{grid}}^2 . \quad (10)$$

Only $\bar{\omega}_{\text{grid}}$ depends on t in Eq. (9). Consequently, the chain rule of calculus can be used to derive:

$$\bar{P}_{\text{fault}} = 2H_{\text{grid}} \bar{\omega}_{\text{grid}} \frac{d}{dt} \bar{\omega}_{\text{grid}} . \quad (11)$$

$\bar{\omega}_{\text{grid}}$ equals 1 in steady state conditions and does not significantly change during transient states. Accordingly, we replace:

$$\bar{\omega}_{\text{grid}} \approx 1 . \quad (12)$$

Inserting in Eq. (11) and rearranging leads to:

$$\frac{d}{dt} \bar{\omega}_{\text{grid}} \approx \frac{\bar{P}_{\text{fault}}}{2H_{\text{grid}}} . \quad (13)$$

In absolute quantities, frequency and angular velocity are proportional.

$$\omega = 2\pi f . \quad (14)$$

The same applies for related quantities. Furthermore, related angular velocity and related frequency are referred to their rated equivalents:

$$\bar{\omega} = \frac{\omega}{\omega_{\text{rated}}} , \quad (15)$$

$$\bar{f} = \frac{f}{f_{\text{rated}}} \quad (16)$$

This delivers the rated value 1 for the related quantities:

$$\bar{\omega}_{\text{rated}} = \bar{f}_{\text{rated}} = 1. \quad (17)$$

This leads to the conclusion:

$$\bar{\omega} = \frac{\omega}{\omega_{\text{rated}}} = \frac{2\pi f}{2\pi f_{\text{rated}}} = \bar{f}. \quad (18)$$

The frequency gradient after a disturbance in a system dominated by directly coupled synchronous generators can consequently be estimated with a simple formula:

$$\frac{d}{dt} \bar{f} \approx \frac{\bar{P}_{\text{fault}}}{2H_{\text{grid}}}. \quad (19)$$

2.4. RoCoF in power systems with high feed-in by inverters

With Eq. (18) it gets clear, why RoCoF has become an important research topic during recent years. With less directly coupled synchronous generation in the system, H_{grid} decreases significantly for the generation of the same active power. H_{grid} is inverse proportional to the RoCoF occurring after a fault, which leads to high RoCoF values in such systems.

Several techniques to compensate for this drawback have been developed in recent years. For wind-dominated systems, a frequency response study can be found in [8]. Other researchers concentrate on FACTS devices, such as synchronous condensers to stabilize the power system [9]. Also, HVDC lines can be used to significantly support systems with low inertia [10].

At the same time, synchronous generators still provide the grid frequency and play an important role in stabilizing power systems after incidents with their directly coupled inertia. The easiest way to keep RoCoF rates after severe grid faults within acceptable ranges is to take care of avoiding inadvertent losses of generation or load or even cascade trips.

Therefore, it is important to know for all synchronous generators relevant for the stability of a power system, which RoCoF events they can compensate.

3. Methodology

For the analysis of effects of severe grid faults on generators, a generator model is necessary that comprises the main components as shown in Fig. 3.

In [20], the model setup for synchronous generators for transient stability studies is described, but no information on control system modelling is given.

Within this section, it is, therefore, derived how the generator model and the control and excitation system model for the studies must be structured. Furthermore, it is shown which possibilities to analyze protection system reactions exist.

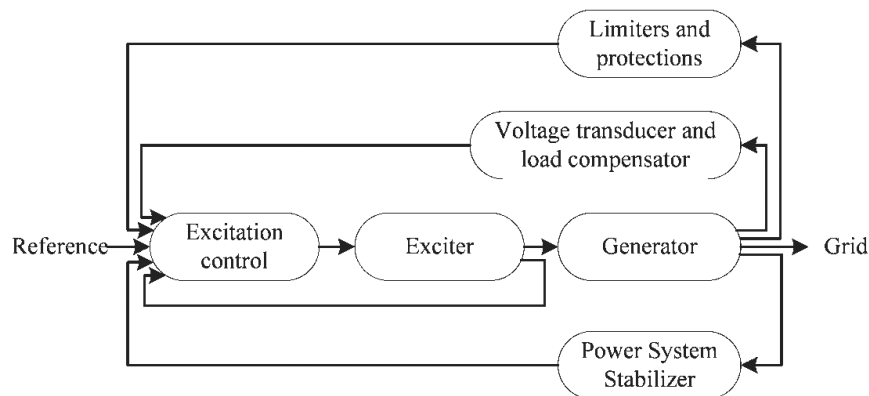


Fig. 3. Main components of generator excitation and control systems

3.1. Generator model

To evaluate the effect of a severe grid failure on a synchronous generator, the following electrical quantities have to be analyzed at first [11]:

- electromagnetic torque in the air gap of the generator T_{el} ;
- pole angle j ;
- active power P ;
- reactive power Q ;
- stator currents;
- stator voltages;
- excitation voltage;
- excitation current;
- rotor speed;
- overall damper current.

For many grid faults, including RoCoF events, a $dq0$ transformed model of the generator is sufficient. For the theory and expanding of the $dq0$ – or Park – transformation, see [6]. For limits of this approach, see e.g. [12].

The parameters for Park models can be determined with tests according to [19]. For existing generators, utilities often have these parameters at hand.

3.2. Control system modelling approach

For transient stability studies, it is of high importance to implement the control system in the system model. For existing generators, there is often only a reference available to corresponding models in the IEEE standard 421.5 [13] together with information, which parameters need to be implemented for stability studies.

The control system model needs at least the following main structures:

- automated voltage regulator (AVR);
- power system stabilizer (PSS);
- turbine governing control (Governor).

Furthermore, it is highly recommendable to implement a model of the underexcitation limiter (UEL), if implemented, because detailed analyses show, that during underexcited operation (leading power factor) and dropping frequency, stability limits can be violated [6].

To implement the turbine governor, models as presented in [14] are often used, if parameters are available.

The question is, if a model of a turbine, generator, and control system, set up with such data is capable of realistically simulating severe grid faults with a high RoCoF. This is evaluated within Section 4.

3.3. Protection system evaluation

With regard to the protection system, three options need to be differentiated.

1. Parametrized protection system model available
2. COMTRADE device installed on the machine
3. Test reports of the protections system available

In the first case, the protection system can be implemented directly in the generator model and a direct evaluation is possible. Especially for existing generators, this will only seldom be the case.

In the second case results from dynamic studies can be transferred to the COMTRADE standard according to IEC 60255-24 [15] and copied directly to the protection system of the synchronous generator. In this way it is possible to evaluate if, at what time, and due to which protection function the system disconnects the generator from the system.

The third case is typical for older generators. In test reports, information can be found, which protection functions are installed and how they are parametrized. How an evaluation of the protection system actuation can be performed in this case is detailed in [16].

4. Control system models

In this section, at first, some details of a validated control system model are discussed for an example generator with $S = 500$ MVA. From this model, a structure in a modelling depth according to the IEEE Standard [13] is derived. The generator model has the following parameters (Table 1):

A more detailed approach is shown in Fig. 4 below. Only the main voltage control loop is depicted. It can be seen that several supplementary controls are implemented in addition to the PSS to achieve a realistic behaviour of the model. The structure of the PSS and the supplementary controls are not shown.

The underexcitation limiter (UEL) is a PQ limiter and produces the dynamic negative ceiling value DNCL. It feeds into a high value gate (HV) that receives the value from the PSS also. The value that is higher passes the link. That leads to a behaviour that immediately kills the voltage setpoint value generated by the PSS and replaces it with the value of the UEL as soon as the latter is higher. Thus, a very quick reaction on violations of the underexcitation limit of the generator is possible.

Similarly, the overexcitation limiter (OEL) feeds into a low value gate (LV) in addition to the value that stems from the HV gate mentioned above.

Table 1. Parameters of synchronous generator model

Parameter name	Value	Unit
Rated apparent power S_n	500	MVA
Rated stator voltage U_n	21	kV
Rated frequency f_n	50	Hz
Rated power factor p.f.	0.80	–
Rated speed	3 000	rpm
Inertia time constant of whole shaft length H based on 500 MVA	6.34	MWs/MVA
Direct axis synchronous reactance (unsat.) X_d	2.14	p.u.
Direct axis transient reactance (unsat.) X_d'	0.35	p.u.
Direct axis sub-transient reactance (unsat.) X_d''	0.27	p.u.
Quadrature axis synchronous reactance (unsat.) X_q	2.05	p.u.
Quadrature axis transient reactance (unsat.) X_q'	0.57	p.u.
Quadrature axis sub-transient reactance (unsat.) X_q''	0.29	p.u.
Saturation factor at 1.0 p.u. stator voltage	0.062	–
Saturation factor at 1.2 p.u. stator voltage	0.208	–

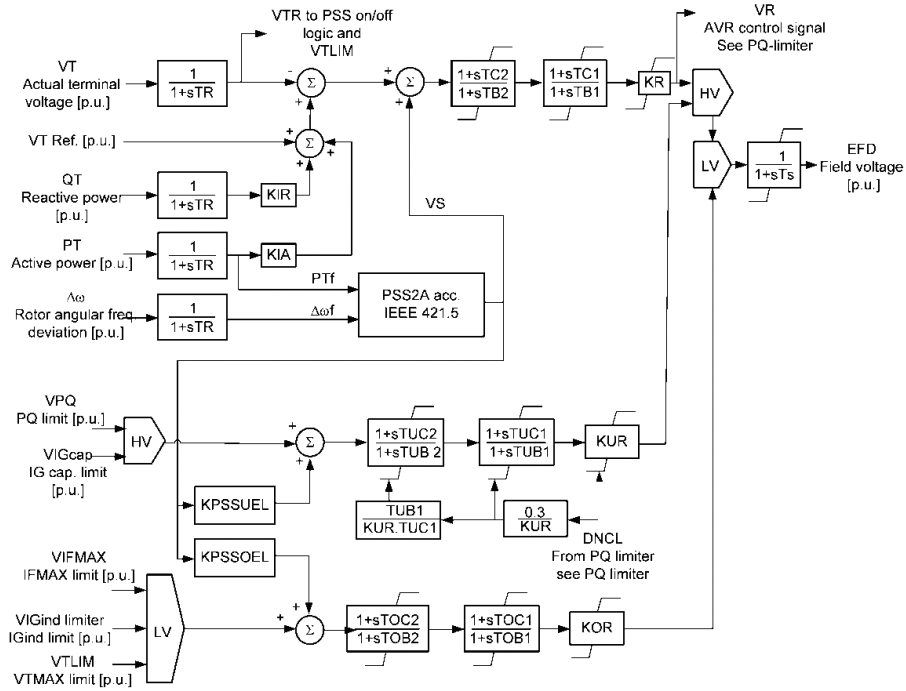


Fig. 4. Detailed excitation system model

The AVR model corresponding to IEEE 421.5 [13] is shown in Fig. 5. It can be seen that a PSS is included. The structure of the PSS is not shown here to keep the paper short. No further supplementary controls are implemented.

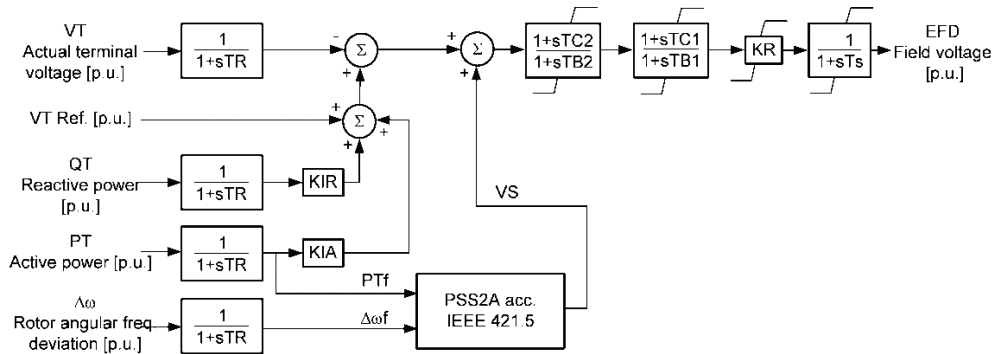


Fig. 5. AVR in a modelling depth corresponding to IEEE 421.5

Consequently, the structure according to IEEE 421.5 [13] can only produce valid results as long as the underexcitation or overexcitation limits are not violated, respectively.

5. Dynamic performance of generator models

In this chapter, results are presented to investigate the influence that the modelling depth of the control system has on the dynamic performance of a synchronous generator.

Results from 2 RoCoF studies are presented:

1. Results from a RoCoF study on one synchronous generator with a detailed control system model are compared with those from the same generator with a control system model according to [13].
2. The same RoCoF study is conducted for nine different generators, two of which are modelled in detail and seven with a structure according to [13].

A frequency trace is inserted into the system with a grid model as shown in Fig. 6.

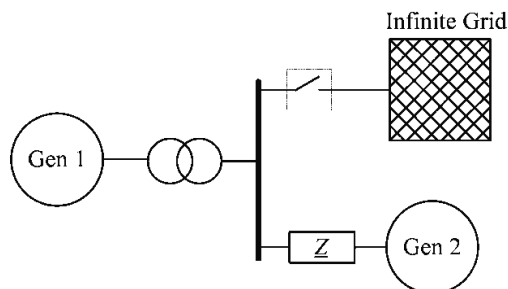


Fig. 6. Power system model for RoCoF study

Gen 1 is the generator under analysis with the parameters as listed in Table 1 above.

The infinite grid helps the software to determine the starting point for the pole angle. It gets disconnected at $t = 0$ s. Gen 2 has a high rated apparent power and a low inertia constant H . Gen 2 impresses the frequency on Gen 1. For that purpose, it has the same impedance as the short circuit impedance of the original power system at the connection point. For further details on the modelling of substitute grids for RoCoF studies, see [6].

In Fig. 7, resulting active power, reactive power, and excitation voltage for one frequency transient are shown.

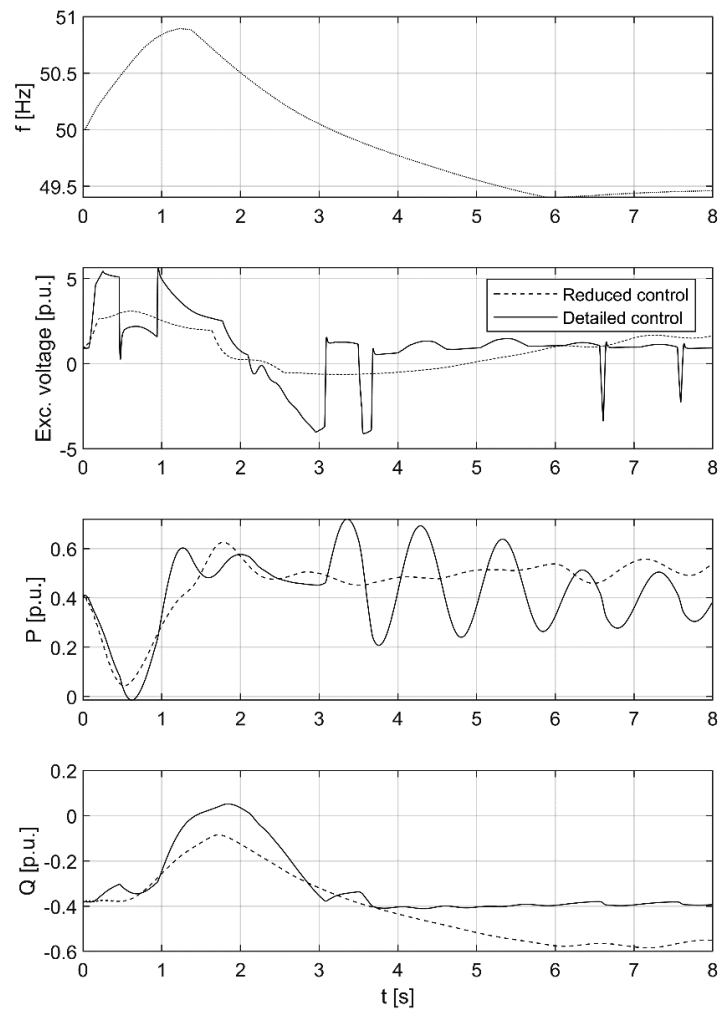


Fig. 7. Comparison of standard and detailed control system model

It can clearly be seen that the detailed structure acts much faster than the controller according to standard [13].

Of specific interest is the reactive power output of the standard model, which goes far beyond the underexcitation limit. The results for the standard controller indicate that the disconnection of the generator by the underexcitation protection needs to be feared. The results for the detailed structure show the opposite: The underexcitation limit is obeyed. This is the expected result according to the structure of the control system implemented, as detailed above.

Anyway, as underexcitation limiters typically measure the impedance instead of the reactive power [17], it is a question of precise coordination of the underexcitation limiter with the underexcitation protection, if even the results derived with the detailed model indicate an actuation of the underexcitation protection. Further details on the analysis of the protection system in such cases can be found in [16].

Because the reactive power results turn out to be a crucial indicator for the performance of the different control structures, results for nine different generators are presented in Fig. 6. The frequency transient is the same as in Fig. 5. The generators have the following basic properties (Table 2):

Table 2. Basic data of synchronous generators

No.	Type	Rated apparent power S_{Gen}	Control system
1	ST	360 MVA	Standard
2	ST	320 MVA	Standard
3	ST	170 MVA	Standard
4	ST	180 MVA	Standard
5	ST	120 MVA	Standard
6	CCGT	500 MVA	Detailed
7	CCGT	500 MVA	Detailed
8	OCGT	70 MVA	Standard
9	Salient pole hydro turbine	30 MVA	Standard

The results in Fig. 8 show that for generators 3, 4, 5, and 9, the underexcitation limit is violated for a longer time period. All these generators are modelled with standard controllers.

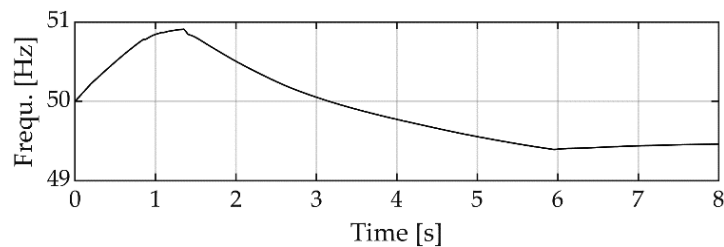


Fig. 8. Reactive power output for different generators

Results from further cases are discussed in [6] undermining that the underexcitation limit is the weak spot of synchronous generators with regard to severe frequency transients.

The controllers presented in [13] can consequently only be used for transient dynamic studies with a high RoCoF with limited accuracy. An indication of potential problems is nevertheless possible.

6. Conclusions

This publication shows how synchronous generators can be modelled for the analysis of severe frequency transients. The focus lies on a practical approach in cases, where no state-of-the-art models for the generator including excitation control and protection system are available.

It can be concluded that the modelling depth has a significant influence on results from dynamic studies like RoCoF studies. Detailed models should be preferred whenever available. Especially, the implementation of underexcitation and overexcitation limiters with realistic behaviour including high-value gates or similar for immediate activation of the limiters is necessary. If not so, it has to be considered, when problems occur, that these might originate in limited model accuracy. In this case, further investigations are necessary.

If the underexcitation limit is violated according to simulation results even with detailed, validated models, this is a question of precisely coordinating the different supplementary controls. It can be of help in this case to change settings of the power system stabilizer (PSS). Approaches for this are presented in [22] and in [23].

References

- [1] European Parliament, European Council, *Directive 2009/28/EC of the European Parliament and of the Council of 23 April 2009*, Official Journal of the European Union, L 140, pp. 16–62 (2009).
- [2] VDE-AR-N 4120:2018-11, *Technical Connection Rules for High-Voltage* (2018).
- [3] Ziping Wu, Wenzhong Gao, Tianqi Gao, Weihang Yan, Huaguang Zhang, Shijie Yan, Xiao Wang, *State-of-the-art review on frequency response of wind power plants in power systems*, Journal of Modern Power Systems and Clean Energy 6.1, ISSN 2196-5420, pp. 1–16 (2018), DOI: [10.1007/s40565-017-0315-y](https://doi.org/10.1007/s40565-017-0315-y).
- [4] O’Sullivan J., Rogers A., Flynn D., Smith P., Mullane A., O’Malley M., *Studying the Maximum Instantaneous Non-Synchronous Generation in an Island System; Frequency Stability Challenges in Ireland*, IEEE Transactions on Power Systems 29.6, ISSN 0885-8950, pp. 2943–2951 (2014), DOI: [10.1109/TPWRS.2014.2316974](https://doi.org/10.1109/TPWRS.2014.2316974).
- [5] Lambrecht D., Kulig T., *Torsional Performance of Turbine Generator Shafts Especially Under Resonant Excitation*, IEEE Transactions on Power Apparatus and Systems PAS-101.10, ISSN 0018-9510, pp. 3689–3702 (1982), DOI: [10.1109/TPAS.1982.317054](https://doi.org/10.1109/TPAS.1982.317054).
- [6] Assenkamp A., *Methods to Assess the Rate of Change of Frequency Withstand Capability of Large Power Plants*, Cuvillier Verlag Göttingen, ISBN 978-3-73697-087-8 (2019).
- [7] Doheny D., Conlon M., *Investigation into the local nature of rate of change of frequency in electrical power systems*, 2017 52nd International Universities Power Engineering Conference (UPEC), pp. 1–6 (2017), DOI: [10.1109/UPEC.2017.8231982](https://doi.org/10.1109/UPEC.2017.8231982).

- [8] Nahid-Al-Masood, Modi N., Saha T.K., Yan R., *Investigation of nonsynchronous penetration level and its impact on frequency response in a wind dominated power system*, 2016 IEEE Power and Energy Society General Meeting (PESGM), pp. 1–5 (2016), DOI: [10.1109/PESGM.2016.7741587](https://doi.org/10.1109/PESGM.2016.7741587).
- [9] Ha Thi Nguyen, Guangya Yang, Nielsen A.H., Jensen P.H., *Frequency stability improvement of low inertia systems using synchronous condensers*, 2016 IEEE International Conference on Smart Grid Communications (SmartGrid-Comm), pp. 650–655 (2016).
- [10] Huang J., Preece R., *HVDC-based fast frequency support for low inertia power systems*, 13th IET International Conference on AC and DC Power Transmission (ACDC 2017), pp. 1–6 (2017).
- [11] Assenkamp A., Hoffmann R., Kreischer C., Exnowski S., *Simulative Analyses of Dynamical Behaviour of Steam-Powered Turbo generators during Power System Incidents with a higher Rate of Change of Frequency*, IET RTDN (2017), 24 (6–246)(6), ISSN 978-1-78561-662-4, pp. 137–142 (2018), DOI: [10.1049/cp.2017.0343](https://doi.org/10.1049/cp.2017.0343).
- [12] Kreischer C., Kulig S., Göbel C., *Applicability of Park transformation for the analysis of transient performance during subsynchronous resonances*, Archives of Electrical Engineering, vol. 62, no. 3, pp. 401–415, ISSN 1427-4221 (2013), DOI: [10.2478/ae-2013-0032](https://doi.org/10.2478/ae-2013-0032).
- [13] IEEE Std 421.5-2016, *IEEE Recommended Practice for Excitation System Models for Power System Stability Studies*, pp. 1–207 (2016).
- [14] Pouyan Pourbeik *et al.*, *Dynamic Models for Turbine-Governors in Power System Studies*, Technical Report PES TR-1, IEEE Power and Energy Society (2013).
- [15] IEC 60255-24, *Measuring relays and protection equipment – Part 24: Common format for transient data exchange (COMTRADE) for power systems* (2013).
- [16] Assenkamp A., Kreischer C., Kulig S., *Capability of synchronous machines to ride through events with high ROCOF*, Archives of Electrical Engineering, vol. 68, no. 2, pp. 325–339, ISSN 1427-4221 (2019), DOI: [10.24425/ae.2019.128271](https://doi.org/10.24425/ae.2019.128271).
- [17] Geoff Klempner, *Handbook of Large Turbo-Generator Operation and Maintenance* (IEEE Press Series on Power Engineering 91), Wiley, ISBN 978-1119389767, 3rd edition (2017).
- [18] Lambrecht D., Kulig T., *Torsional Performance of Turbine Generator Shafts Especially Under Resonant Excitation*, IEEE Transactions on Power Apparatus and Systems PAS-101.10, pp. 3689–3702, ISSN 0018-9510 (1982), DOI: [10.1109/TPAS.1982.317054](https://doi.org/10.1109/TPAS.1982.317054).
- [19] IEEE Std 115-2009, *IEEE Guide for Test Procedures for Synchronous Machines – Part I Acceptance and Performance Testing – Part II Test Procedures and Parameter Determination for Dynamic Analysis*, pp. 1–219 (2009), DOI: [10.1109/IEEESTD.2010.5953453](https://doi.org/10.1109/IEEESTD.2010.5953453).
- [20] IEEE Std 1110-2002, *IEEE Guide for Synchronous Generator Modeling Practices and Applications in Power System Stability Analyses* (2003).
- [21] Serban E., Ordonez M., Pondiche C., *Voltage and Frequency Grid Support Strategies Beyond Standards*, IEEE Transactions on Power Electronics 32.1, pp. 298–309, ISSN 0885-8993 (2017), DOI: [10.1109/TPEL.2016.2539343](https://doi.org/10.1109/TPEL.2016.2539343).
- [22] Kerperin A., Assenkamp A., Kreischer C., *PSS Modification to stabilize synchronous machines during events with high rate of change of frequency*, 2019 IEEE PowerTech, Milan, ISBN 978-1-5386-4722-6 (2019), DOI: [10.1109/PTC.2019.8810981](https://doi.org/10.1109/PTC.2019.8810981).
- [23] Nocon A., Paszek S., *Analysis of power system stabilizer Pareto optimisation when taking into account the uncertainty of power system mathematical model parameters*, Archives of Electrical Engineering, vol. 60, no. 4, pp. 385–398, ISSN 1427-4221 (2011), DOI: [10.2478/v10171-011-0033-4](https://doi.org/10.2478/v10171-011-0033-4).